THE JOURNAL OF PHYSICAL CHEMISTRY Letters

LETTER

pubs.acs.org/JPCL

Persistent Covalency and Planarity in the $B_nAl_{6-n}^{2-}$ and $LiB_nAl_{6-n}^{-}$ (n = 0−6) Cluster Ions

Mioy T. Huynh and Anastassia N. Alexandrova*

Department of Chemistry and Biochemistry, University of California, Los Angeles, Los Angeles, California 90095-1569, United States

Supporting Information

ABSTRACT: The chemical bonding being covalent, metallic, or mixed reflects in the structure and properties of solids. How does this play out on the small cluster scale? We report on the interplay between covalent and strongly delocalized bonding in the series of mixed boron−aluminum cluster ions, $B_nAl_{6-n}^{2-}$ (n = 0−6), and their lithium salts and show that covalent bonding is an extraordinarily resilient effect that governs the cluster shape more than the delocalized bonding does. The covalent bonding achieved only through the direct B−B interactions is persistent in the considered clusters down to the smallest concentrations of B atoms. As a result, clusters remain planar, and the quality of the delocalized bonding is unavoidably compromised. We explain this trend on the basis of the s−p hybridization of atomic orbitals affordable in the B versus Al atoms. The found effect may be general and not specific to the considered systems.

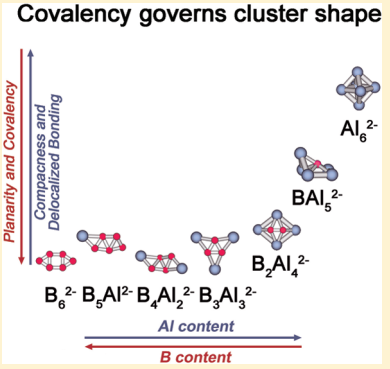

SECTION: Dynamics, Clusters, Excited States

Covalent and metallic bonding in solids profoundly impacts their properties, which have been widely exploited by humankind since ancient times. More exotic types of chemical bonding in solids are also known, for example, mixed ionic-covalent bonding characteristic of certain ceramics and perovskites. The basic classification of materials according to the type of chemical bonding in them goes together with our intuition about their structure and properties. However, it is less understood how similar covalent-metallic bonding interplay manifests itself at the small cluster size. As modern technology evolves toward nano- and subnanoscales, it becomes increasingly important to have a qualitative understanding of the chemical bonding in clusters to have intuition about them and predict their properties and shapes, much as we are capable of doing for extended solids and surfaces.

Recent theoretical and experimental discoveries have moved us closer to such understanding. Among a few successful examples are clusters of boron and aluminum.[1−8] Despite the apparent electronic structure similarity of B ($[He]2s^22p^1$) and Al ($[Ne]3s^23p^1$), their clusters adopt very different structures, except at the smallest cluster size of 1−5 atoms. Specifically, all-B clusters are planar,[1−4] whereas all-Al clusters are closed 3-D.[5−8] Consider the two species, the B_6^{2-} and Al_6^{2-} anions, observed experimentally in the form of lithium salts, LiB_6^{-}[2,3] and $LiAl_6^{-}$.[8] In Figure 1, the global minimum forms of the B_6^{2-} and Al_6^{2-} ions are shown, along with the details of chemical bonding in them. Both clusters can be described as formed by two triangular units, B_3^{-} and Al_3^{-}. In the case of B_6^{2-} the two units bind in plane, forming a planar D_{2h} (^1A_g) cluster, whereas for Al_6^{2-}, the two units bind in 3-D forming an octahedron, O_h ($^1A_1'$). Upon coordination of Li^+, the shapes and nature of the chemical bonding in the ions are preserved.

Detailed analysis of the chemical bonding in these clusters can be found in the literature,[2,3,8] and here we will present only a brief overview of these findings and strategically compare the two, thus posing the question to be answered. The reason for the observed structural difference is explainable on the basis of the affordability of s−p hybridization of atomic orbitals (AOs) in B versus Al. In B, the 2s−2p energy separation is smaller, and the hybridization is more attainable. This hybridization is adopted to achieve 2c−2e B−B covalent bonding. Indeed, the HOMO-9, HOMO-8, HOMO-7, HOMO-6, HOMO-5, and HOMO-1 in B_6^{2-} can be localized, as six covalent bonds along the periphery of the planar cluster. The rest of the chemical bonding in the system is realized through delocalized MOs (the HOMO, HOMO-2, HOMO-3, and HOMO-4), and the cluster was characterized as doubly antiaromatic (σ and π) because of the population of the π- and σ-subsets of delocalized MOs by four electrons each (Figure 1A).[6]

In Al, the larger nuclear charge favors the AOs of lower angular momentum, the 3s−3p energy separation increases, and mixing is discouraged. As a result, in contrast with B_6^{2-}, no directional covalent bonding occurs in Al_6^{2-}. The HOMO-9, HOMO-8, HOMO-7, HOMO-6, HOMO-5, and HOMO-2 are simply combinations of nonoverlapping 3s AOs on Al atoms, whose net bonding effect in the cluster is zero. The entire bonding in Al_6^{2-} thus comes from the delocalized MOs: the HOMO and HOMO-1 (Figure 1B). Because of the population of these MOs, the system was previously characterized as 3-D aromatic.[8]

Received: June 27, 2011
Accepted: July 22, 2011
Published: July 22, 2011

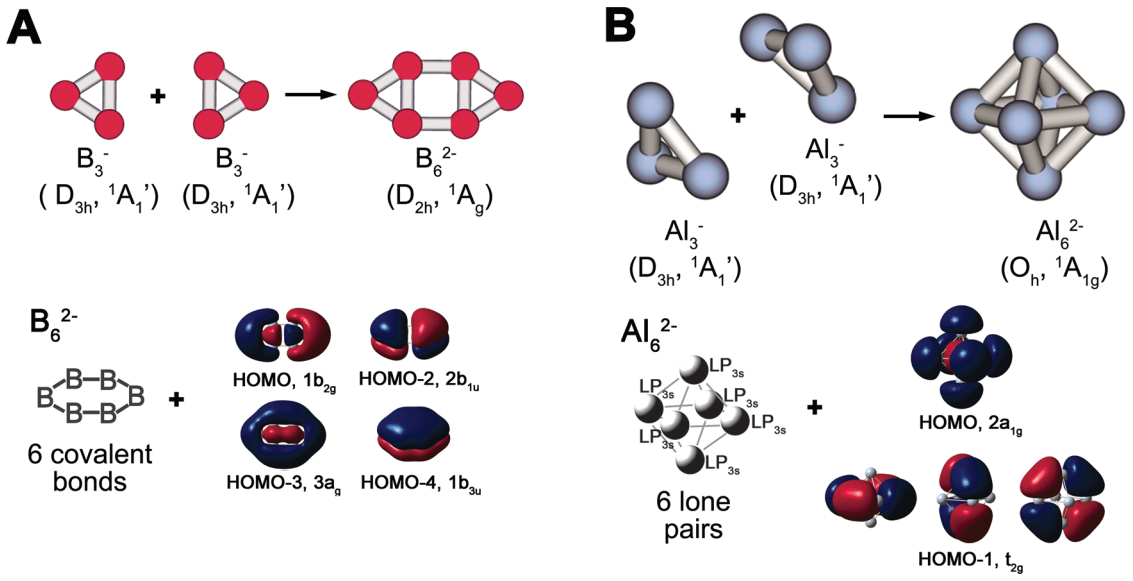

Figure 1. B_6^{2-} (A) versus Al_6^{2-} (B): In the all-B cluster, six valence MOs are localizable as six 2c−2e B−B bonds along the periphery of the cluster, and the rest of MOs are shared by all atoms, that is, delocalized. In the all-Al cluster, six valence MOs are localizable as six 3s lone pairs on Al atoms, and the rest of the MOs are delocalized. Both clusters can be seen as formed by two triatomic units, except that in Al_6^{2-} the units come together in 3-D to maximize the delocalized overlap, whereas in B_6^{2-} the units come in plane to allow for covalent bonding but compromise the delocalized bonding.

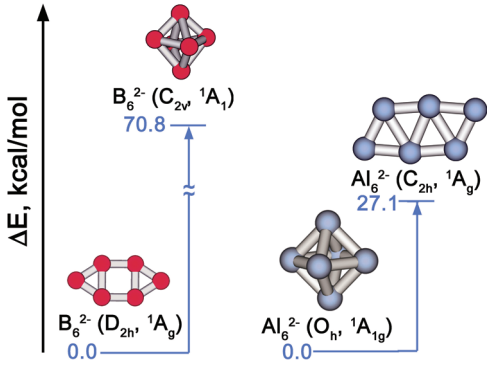

Figure 2. Relative energies of the planar and 3-D isomers of B_6^{2-} and Al_6^{2-} (B3LYP[9−11]/6-311+G*[12,13] level), illustrating how covalent bonding is favored in 2-D structures, whereas delocalized overlap is favored in 3-D.

Notice that when Al_6^{2-} adopts a 3-D structure, the overlap of completely delocalized MOs of the two Al_3^- units is more extensive and constructive. If a planar structure is formed, then this delocalized overlap is compromised. This is illustrated by the energy difference between the 3-D global minimum and the planar C_{2h} structure of Al_6^{2-}, which is 27.1 kcal/mol. (The D_{2h} structure analogous to that of B_6^{2-} is not a minimum for Al_6^{2-}.) Even though the delocalized overlap is suboptimal in 2-D, the planar structure is still adopted in B_6^{2-}. The reason is that the covalency achievable in 2-D more than compensates for the deficiency in delocalized bonding. The compact C_{2v} structure of B_6^{2-} lays 70.8 kcal/mol higher in energy than the planar global minimum, as shown in Figure 2. (The O_h structure is a saddle point for B_6^{2-}.)

Putting it all together, covalent bonding is attainable in 2-D structures, whereas no covalent bonding can be achieved in 3-D; at the same time, delocalized overlap is favored in 3-D, and suboptimal in 2-D. Hence, what becomes clear is that covalent and delocalized bonding are opposite effects in governing cluster shapes. Which of the two chemical bonding effects is qualitatively more significant? In other words, how much of an impact on cluster shape and properties can one expect from each of them for a particular cluster composition? Understanding this would turn delocalization and covalency into rational cluster design tools. Let us now set covalency and delocalized bonding against each other using a specific cluster series, $B_nAl_{6-n}^{2-}$ and $LiB_nAl_{6-n}^{-}$ (n = 0−6), as a model system. We probe how many doping Al atoms it would take for the delocalized bonding to be strong enough to override the preference for directional covalent bonding, that is, to switch from planar to globular 3-D structure of the ions.

The found global minimum structures of the doubly charged ions and their Li salts are shown in Figure 3. These structures were found via our in-house ab initio gradient embedded genetic algorithm code (GEGA)[19,20] (Theoretical Methods section), and separate searches were performed for singlets and triplets. All lowest-energy isomers of these species are singlets, and the triplets are significantly higher in energy. The studied doubly charged ions are unstable against the ejection of an electron, just like the parent B_6^{2-} and Al_6^{2-} ions (the phenomenon well known in the chemistry if cluster ions[1,21]). However, the Li salts are stable. The first vertical electron detachment energies, corresponding to the removal of an electron from the HOMO range from 2.54 to 4.08 eV, as calculated at the MP2/6-311+G(2df) level of theory. Salts of B_6^{2-} and Al_6^{2-} have been observed experimentally, and our results suggest that all salts in the considered series are also obtainable at least in the gas phase. The charge distribution in the salts is such that Li holds the charge of +0.5 to +0.7, that is, mostly transfers an electron to the cluster ion and binds to it ionically (Table 1). An additional observation can be made that the structures of the isolated ions and the ions inside the Li salts are very similar. Hence, the following discussion is focused on the chemical bonding in the stand-alone doubly charged ions, which are apparently perturbed little by the presence of Li^+.

dx.doi.org/10.1021/jz200865u |J. Phys. Chem. Lett. 2011, 2, 2046–2051

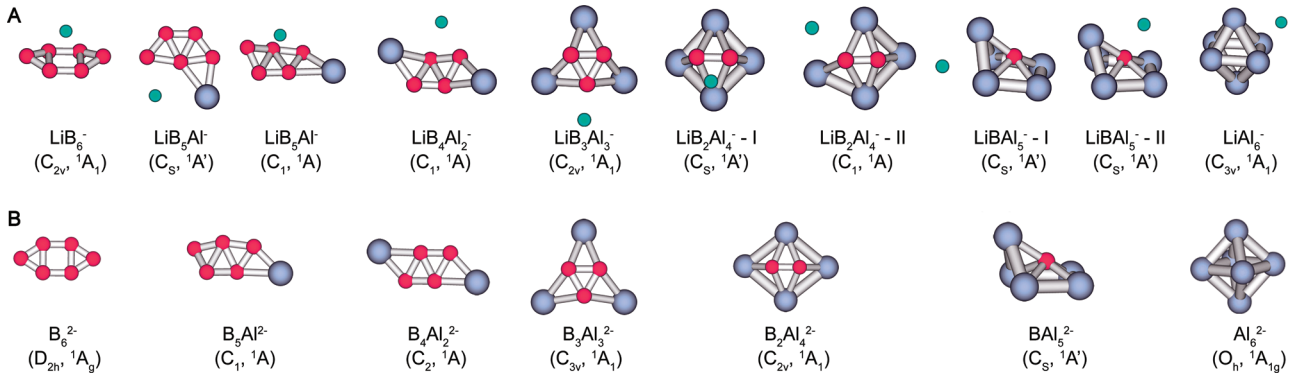

Figure 3. Global minima and lowest energy isomers of the $LiB_nAl_{6-n}^-$ ionic salts (A) and the $B_nAl_{6-n}^{2-}$ ions (B) found with GEGA and refined at the MP2/6-311+G* level of theory. In cases where two isomers of the same species are shown, their energy difference was found to be insignificant across theoretical methods. The known all-B and all-Al ions are shown for completeness. Color scheme: red, B; purple, Al; green, Li. The geometries of the anions are mostly unchanged upon coordination of the metal.

Table 1. Natural Bond Order (NBO)[14−18]//B3LYP/6-311+G* Average Charges on Atoms of the Same Type, Averaged B−B Distances, and Averaged Populations of the 2s AO on B and 3s AO on Al in the $LiB_nAl_{6-n}^-$ Salts

species	Q(Li)	$Q(B)_{av}$	$Q(Al)_{av}$	$R(B-B)_{av}$, Å	$Pop(2s\ AO_B)_{av}$[a]	$Pop(3s\ AO_{Al})_{av}$[a]
LiB_6^- (C_{2v}, $^1A_1$)	+0.700	−0.283	n/a	1.566	0.90	n/a
LiB_5Al^- (C_s, $^1A'$)	+0.500	−0.169	+0.343	1.669	1.03	1.55
LiB_5Al^- (C_1, ^1A)	+0.677	−0.200	+0.321	1.619	0.94	1.65
$LiB_4Al_2^-$ (C_1, ^1A)	+0.739	−0.346	+0.324	1.621	0.99	1.64
$LiB_3Al_3^-$ (C_s, $^1A'$)	+0.471	−0.920	+0.763	1.643	1.04	1.58
$LiB_2Al_4^-$ (C_s, $^1A'$) − I	+0.715	−1.797	+0.720	1.576	1.14	1.44
$LiB_2Al_4^-$ (C_1, ^1A) − II	+0.456	−1.645	+0.709	1.608	1.15	1.56
$LiBAl_5^-$ (C_s, $^1A'$) − I	+0.448	−2.988	+0.508	n/a	1.33	1.44
$LiBAl_5^-$ (C_s, $^1A'$) − II	+0.669	−2.835	+0.433	n/a	1.38	1.50
$LiAl_6^-$ (C_{3v}, $^1A_1$)	+0.380	n/a	−0.230	n/a	n/a	1.43

[a] Natural population of the s AOs serves as a qualitative metric on the s−p hybridization, even though in reality the picture is more complicated because of intracluster charge transfer.

From Figure 3, one may clearly see a gradual progression from planar to 3-D structures as the number of Al atoms in the clusters increases. However, the onset of this structural change is late in the series: only as the content of Al atoms reaches four in the six-atomic cluster ion does the structure become 3-D. Al−Al bonding is completely discouraged before then. It is also worth remarking that DFT calculations predict the $B_2Al_4^{2-}$ ion to be still planar and the 2-D to 3-D transition to happen only at BAl_5^{2-}, whereas at MP2[41−43] and CCSD(T)[44−49] levels the transition does happen at $B_2Al_4^{2-}$. In all clusters containing two or more B atoms, short covalent B−B bonds are formed, as predicted by the NBO analysis. This fact is illustrated by consistently short (ca. 1.6 Å) averaged interatomic B−B distances in all species (Table 1).

The global minimum structure of B_5Al^{2-}, stand-alone and inside the LiB_5Al^- salt, is planar. It contains the known B_5 unit (approximately C_{2v} in symmetry).[1] The Al atom is bound to the B_5-unit in plane, and in the salt, there are two isoenergetic isomers that differ in the position of Al. Al donates a total of 0.3 electrons to the B_5 unit (Table 1) and forms a weak ionic bond to it. No directional bonding between the B-core and Al can be detected. From the molecular orbital (MO) picture (Figure 1S in the Supporting Information), it can be seen that the mixing between AOs on Al and MOs on the B_5 unit exists, but it is minimal. The species are remarkably similar to low-lying isomers of B_6^{2-} although structurally frustrated. In this cluster, covalency inherent for B completely dictates the shape.

The $B_4Al_2^{2-}$ ion is very similar to B_5Al^{2-}: it is also planar, with two Al atoms coordinated in plane to the known B_4 unit.[1] The Al atoms are located in the cluster as far apart from one another as possible. The total amount of charge transfer from Al atoms to the B-core (0.6 electrons) is double that in B_5Al^{2-}, again illustrating the similarity between these species. Planarity and covalency so far persist.

The $B_3Al_3^{2-}$ ion, containing an equal number of B and Al atoms, is in a way the most remarkable in the series. It has a B_3 triangular core, which is a very prominent, covalently bound motif in B clusters.[1] The Al atoms are bound to its periphery largely ionically, with a significant Al−B charge transfer. There is no Al−Al bonding; furthermore, Al atoms coulombically repulse each other. The structure overall is quasi-planar, guided by the covalent B_3 core. Why is it that charge transfer from Al to B_3 preferred over Al−Al bonding? The reason for this preference is in the relative electronegativities of the two elements and the electronic structure of the B_3 core (Figure 4). The HOMO-6 and HOMO-5 are MOs that are localizable as 2c−2e covalent B−B bonds, as in the B_3^- cluster previously reported.[22] The HOMO-2 is a π-MO. Populated by two electrons, it makes the cluster obey the $(4n + 2)$ Hückel's rule, and the cluster thus possesses

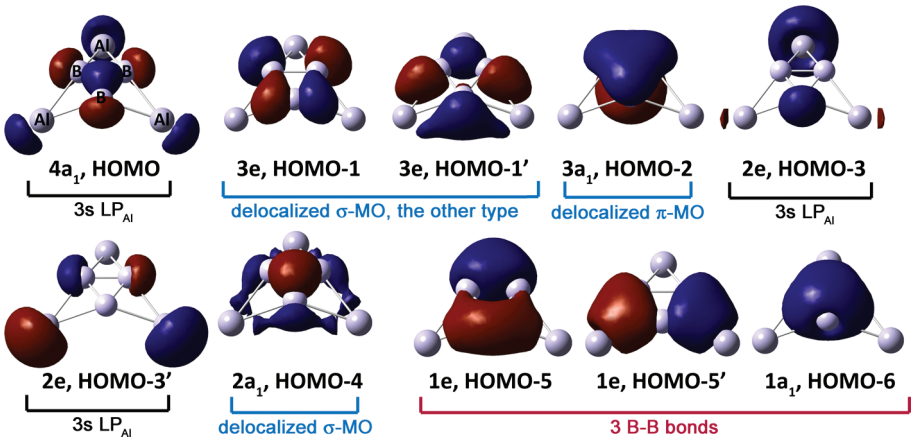

Figure 4. Valence MOs of the $Al_3B_3^{2-}$ ion. The primary contributions to each MO are shown as a qualitative description because some mixing within MOs of the same symmetry always occurs. A delocalized σ-MO of "the other type" is filled in B_3 within this cluster because of charge transfer from Al. All atoms are depicted schematically without designated colors or radii.

π-aromaticity in the B_3 unit, just like the isolated B_3^-.[22] The HOMO-4 is a completely bonding and fully delocalized MO of the σ-character. It is formed by the 2s−2p hybrids on B atoms pointing into the center of the cluster. Because of this MO, the cluster is also σ-aromatic. There is one more doubly degenerate MO that is mainly formed by AOs on B: the HOMO-1. This MO is formed by the B AOs that lay in the plane of the cluster and are orthogonal to those forming the HOMO-4. Their overlap happens on the periphery of the B_3 core. The overlap achieved in the HOMO-1 is the most bonding for this type of AOs because of the symmetry of the cluster. Therefore, the charge transfer from Al allows for this new type of σ-bonding in B_3 to be fulfilled, and it is apparently preferred over Al−Al bonding. It is clear that the structure of $Al_3B_3^{2-}$ allows for both covalent bonding and significant delocalized bonding within B_3. The covalent B−B bonds bring the B atoms closer, and that makes the overlap of all kinds of B AOs more constructive. For this reason, delocalized bonding between B atoms also appears to be stronger than what could be achieved between Al atoms. This is how covalency fights solely delocalized bonding with a double-edged sword, wins, and thus constitutes a more significant bonding effect.

In $B_2Al_4^{2-}$, the two B atoms form a short bond, and the Al atoms are scattered around the B−B core. At the B3LYP/6-311+G* level of theory, there is no bonding between Al atoms, and the cluster is planar. However, at MP2/6-311+G* and CCSD(T)/6-311+G*, Al−Al bonding develops, together with the transition of the geometry from 2-D to 3-D. The cluster then consists of the B−B diatomic and the square Al_4 unit. At this cluster composition, the balance between covalent bonding and optimal delocalized bonding (achievable in 3-D) is achieved.

Finally, BAl_5^{2-} has a 3-D structure, with prominent Al−Al bonding. In Tables 1S−5S (Supporting Information), selected molecular properties of the species shown in Figure 3 are presented and compared across theoretical methods.

The natural electronic configurations partially reported in Table 1 show the hybridization of AOs, reflected in the degree of covalency affordable in an atom. In all clusters, B atoms exhibit a strong 2s−2p mixing, with a significantly reduced 2s population. Al atoms within the studied clusters exhibit smaller 3s−3p mixing and greater 3s population. This is the origin of the structural preferences that B and Al clusters adopt.

The fact that planar structures persist in the considered cluster series demonstrates that covalency, which is associated with planarity, is an electronic effect largely governing the structure. Stand-alone covalent bonds are strong, and when there is chance to form them in a cluster, it likely will happen. However, additionally, covalency welcomes delocalized bonding that develops on the covalent skeleton (on the B-core, in our case), because covalent bonds bring atoms closer together, and the delocalized overlap of AOs also becomes more constructive. This is illustrated by the significant charge transfer to the B-core within all considered ions (Table 1), which leads to new types of delocalized bonding within the covalent B-core, at the expense of delocalized bonding over the entire cluster possible in 3-D. Therefore, covalent bonding is a strong effect capable of overriding the optimal delocalized overlap through a complicated two-sided mechanism. As an illustration of stronger bonding due to covalency, it is worth mentioning that for the doubly charged ions the cluster binding energy per atom increases linearly with the B content, with R^2 = 0.99 (Table 6S of the Supporting Information). This relative strength of covalent and delocalized bonding effects is most likely general in clusters and important to keep in mind in the design of cluster of desired shapes and properties.

THEORETICAL METHODS

An automated extensive search for the global minima was performed for all discussed clusters, except for B_6^{2-}, B_6Li^-, Al_6^{2-}, and Al_6Li^-, whose structures were known from the literature. The searches were done with our in-house ab initio gradient embedded genetic algorithm (GEGA)[19,20] program at the B3LYP/3-21G level of theory. Separate searches were performed for singlets and triplets. For every structure, three independent runs of the GEGA search were performed. Details of the algorithm can be found elsewhere.[19,20] The population size was 30, and the convergence was considered to be sufficient when the current most stable structure was the same for 20 consecutive iterations. From our experience, GEGA performs exceptionally well for finding the global minima of clusters, as was confirmed in numerous joint theoretical and experimental spectroscopic studies.[1,22−40] The lowest energy isomers found to be within 15 kcal/mol from the global minimum were retained for further consideration. Their geometries and vibrational frequencies were refined at the B3LYP/6-311+G*, MP2/6-311+G*, and

dx.doi.org/10.1021/jz200865u |J. Phys. Chem. Lett. 2011, 2, 2046–2051

CCSD(T)[44−50]/6-311+G* levels of theory. For all global minima, the vertical electron detachment energies were calculated with MP2/6-311+G(2df)//MP2/6-311+G*. The analysis of chemical bonding was done with NBO at the B3LYP/6-311+G* level and MO analysis was done at the HF/3-21G level. In addition, single-point energy calculations at CASSCF(n, m)[51−56]/6-311+G* (n = 4−6, m = 4−6) were carried out for the MP2 geometries to check the validity of the single determinant methods. It was confirmed that all considered species have unequivocally single configuration wave functions, and hence the single reference methods should be reliable. Gaussian 09[57] was used for all calculations and MOLDEN[58] was used for visualization.

■ ASSOCIATED CONTENT

Supporting Information. Molecular properties of the lowest-energy isomers calculated at different levels of theory, structures of competitive isomers, and MO diagrams, and the partial results of the NBO analysis for the doubly charged ions. This material is available free of charge via the Internet at http://pubs.acs.org.

■ AUTHOR INFORMATION

Corresponding Author
*E-mail: ana@chem.ucla.edu.

■ ACKNOWLEDGMENT

We dedicate this publication to Professor Alex Boldyrev (Utah State University), the author of many pioneering works on chemical bonding in clusters and a wonderful mentor of many grateful students, including one of us (A.N.A.), on the occasion of his 60th birthday. This work was supported by the University of California through the Faculty Career Development Award and Faculty Research Grant (A.N.A.) and the URFP Fellowship (M.T.H.).

■ REFERENCES

(1) Alexandrova, A. N.; Boldyrev, A. I.; Zhai, H.-J.; Wang, L.-S. All-Boron Aromatic Clusters as Potential New Inorganic Ligands and Building Blocks in Chemistry. *Coord. Chem. Rev.* **2006**, *250*, 2811–2866 and references therein.

(2) Alexandrova, A. N.; Boldyrev, A. I.; Zhai, H.-J.; Wang, L.-S.; Steiner, E.; Fowler, P. W. Structure and Bonding in B_6^- and B_6: Planarity and Antiaromaticity. *J. Phys. Chem. A* **2003**, *107*, 1359–1369.

(3) Alexandrova, A. N.; Boldyrev, A. I.; Zhai, H.-J.; Wang, L.-S. Electronic Structure, Isomerism, and Chemical Bonding in B_7^- and B_7. *J. Phys. Chem. A* **2004**, *108*, 3509–3517.

(4) Zhai, H.-J.; Alexandrova, A. N.; Wang, L.-S.; Boldyrev, A. I. Hepta- and Octacoordinate Boron in Molecular Wheels of Eight- and Nine-Atom Boron Clusters: Observation and Confirmation. *Angew. Chem., Int. Ed.* **2003**, *42*, 6004–6008.

(5) Boldyrev, A. I.; Wang, L.-S. All-Metal Aromaticity and Antiaromaticity. *Chem. Rev.* **2005**, *105*, 3716–3757 and references therein.

(6) Li, X.; Kuznetsov, A. E.; Zhang, H.-F.; Boldyrev, A. I.; Wang, L.-S. Observation of All-Metal Aromatic Molecules. *Science* **2001**, *291*, 859–861.

(7) Kuznetsov, A. E.; Birch, K. A.; Boldyrev, A. I.; Li, X.; Zhai, H.-J.; Wang, L.-S. All-Metal Antiaromatic Molecule: Rectangular Al_4^{4+} in the $Li_3Al_4^-$ Anion. *Science* **2003**, *300*, 622–625.

(8) Kuznetsov, A. E.; Boldyrev, A. I.; Zhai, H.-J.; Li, X.; Wang, L.-S. Al_6^{2-} - Fusion of Two Aromatic Al_3^- Units. A Combined Photoelectron Spectroscopy and Ab initio Study of $M^+[Al_6^{2-}]$ (M = Li, Na, K, Cu, and Au). *J. Am. Chem. Soc.* **2002**, *124*, 11791–11801.

(9) Parr, R. G.; Yang, W. *Density-Functional Theory of Atoms and Molecules*; Oxford University Press: Oxford, U.K., 1989.

(10) Becke, A. D. Density-Functional Thermochemistry. III. The Role of Exact Exchange. *J. Chem. Phys.* **1993**, *98*, 5648–5652.

(11) Perdew, J. P.; Chevary, J. A.; Vosko, S. H.; Jackson, K. A.; Pederson, M. R.; Singh, D. J.; Fiolhais, C. Atoms, Molecules, Solids, and Surfaces: Applications of the Generalized Gradient Approximation for Exchange and Correlation. *Phys. Rev. B* **1992**, *46*, 6671–6687.

(12) Clark, T.; Chandrasekhar, J.; Spitznagel, C. W.; Schleyer, P. v. R. Efficient Diffuse Function-Augmented Basis Sets for Anion Calculations. III. The 3-21+G Basis Set for First-Row Elements, Li-F. *J. Comput. Chem.* **1983**, *4*, 294–301.

(13) Frisch, M. J.; Pople, J. A.; Binkley, J. S. Self-Consistent Molecular Orbital Methods 25. Supplementary Functions for Gaussian Basis Sets. *J. Chem. Phys.* **1984**, *80*, 3265–3269.

(14) Carpenter, J. E; Weinhold, F. Analysis of the Geometry of the Hydroxymethyl Radical by the "Different Hybrids for Different Spins" Natural Bond Orbital Procedure. *THEOCHEM* **1988**, *169*, 41–62.

(15) Carpenter, J. E. Ph.D. Thesis, University of Wisconsin, Madison, WI, 1987.

(16) Foster, J. P.; Weinhold, F. Natural Hybrid Orbitals. *J. Am. Chem. Soc.* **1980**, *102*, 7211–7218.

(17) Reed, A. E.; Weinhold, F. Natural Bond Orbital Analysis of Near-Hartree-Fock Water Dimer. *J. Chem. Phys.* **1983**, *78*, 4066–4073.

(18) Reed, A. E.; Curtiss, L. A.; Weinhold, F. Intermolecular Interactions from a Natural Bond Orbital, Donor-Acceptor Viewpoint. *Chem. Rev.* **1988**, *88*, 899–926.

(19) Alexandrova, A. N. $H(H_2O)_n$ Clusters: Microsolvation of the Hydrogen Atom via Molecular ab Initio Gradient Embedded Genetic Algorithm (GEGA). *J. Phys. Chem. A* **2010**, *114*, 12591–12599.

(20) Alexandrova, A. N.; Boldyrev, A. I. Search for the $Li_n^{0/+1/-1}$ (n = 5−7) Lowest-Energy Structures Using the ab Initio Gradient Embedded Genetic Algorithm (GEGA). Elucidation of the Chemical Bonding in the Lithium Clusters. *J. Chem. Theory Comput.* **2005**, *1*, 566–580.

(21) Simons, J. Molecular Anions. *J. Phys. Chem. A* **2008**, *112*, 6401–6511.

(22) Zhai, H.-J.; Wang, L.-S.; Alexandrova, A. N.; Boldyrev, A. I.; Zakrzewski, V. G. Photoelectron Spectroscopy and ab Initio Study of B_3^- and B_4^- Anions and Their Neutrals. *J. Phys. Chem. A* **2003**, *107*, 9319–9328.

(23) Zubarev, D. Yu.; Averkiev, B. B.; Zhai, H.-J.; Wang, L.-S.; Boldyrev, A. I. Aromaticity and Antiaromaticity in Transition-Metal Systems. *Phys. Chem. Chem. Phys.* **2008**, *10*, 257–267.

(24) Zhai, H.-J.; Averkiev, B. B.; Zubarev, D. Yu.; Wang, L.-S.; Boldyrev, A. I. δ Aromaticity in $[Ta_3O_3]^-$. *Angew. Chem., Int. Ed.* **2007**, *46*, 4277–4280.

(25) Cui, L. F.; Huang, X.; Wang, L.-M.; Zubarev, D. Yu.; Boldyrev, A. I.; Li, J.; Wang, L. S. Sn_{12}^{2-}: Stannaspherene. *J. Am. Chem. Soc.* **2006**, *128*, 8390–8391.

(26) Alexandrova, A. N.; Koyle, E.; Boldyrev, A. I. Theoretical Study of Hydrogenation of Doubly-Aromatic B_7^-. *J. Mol. Model* **2006**, *12*, 569–576.

(27) Zubarev, D. Yu.; Alexandrova, A. N.; Boldyrev, A. I.; Ciu, L.-F.; Wang, L.-S. On the Structure and Chemical Bonding of Si_6^{2-} and Si_6^{2-} in $NaSi_6^-$ upon Na^+ Coordination. *J. Chem. Phys.* **2006**, *124*, 124305–124305−13.

(28) Wang, L.-M.; Huang, W.; Wang, L. S.; Averkiev, B. B.; Boldyrev, A. I. Experimental and Theoretical Investigation of Three-Dimensional Nitrogen-Doped Aluminum Clusters Al_8N^- and Al_8N. *J. Chem. Phys.* **2009**, *130*, 134303–134303−7.

(29) Averkiev, B. B.; Call, S.; Boldyrev, A. I.; Wang, L. M.; Huang, W.; Wang, L. S. Photoelectron Spectroscopy and Ab Initio Study of the Structure and Bonding of Al_7N^- and Al_7N. *J. Phys. Chem. A* **2008**, *112*, 1873–1879.

(30) Zubarev, D.; Yu., Li, J.; Wang, L.-S.; Boldyrev, A. I. Theoretical Probing of Deltahedral Closo-AuroBoranes $B_xAu_x^{2-}$ (x = 5−12). *Inorg. Chem.* **2006**, *45*, 5269–5271.

(31) Averkiev, B. B.; Zubarev, D. Yu; Wang, L.-M.; Huang, W.; Wang, L.-S.; Boldyrev, A. I. Carbon Avoids Hypercoordination in CB_6^-,

CB_6^{2-}, and $C_2B_5^-$ Planar Carbon-Boron Clusters. *J. Am. Chem. Soc.* **2008**, *130*, 9248–9250.

(32) Sergeeva, A. P.; Zubarev, D. Yu; Zhai, H.-J.; Boldyrev, A. I.; Wang, L.-S. A Photoelectron Spectroscopic and Theoretical Study of B_{16}^- and B_{16}^{2-}: An All-Boron Naphthalene. *J. Am. Chem. Soc.* **2008**, *130*, 7244–7246.

(33) Wang, L.-M.; Huang, W.; Averkiev, B. B.; Boldyrev, A. I.; Wang, L.-S. Theoretical Design of Planar Molecules with a Nona- and Deca-Coordinate Central Atom. *Russ. J. Gen. Chem.* **2008**, *78*, 769–773.

(34) Wang, L.-M.; Huang, W.; Averkiev, B. B.; Boldyrev, A. I.; Wang, L.-S. CB_7^-: Experimental and Theoretical Evidence against Hypercoordination Planar Carbon. *Angew. Chem., Int. Ed.* **2007**, *46*, 4550–4553.

(35) Tiznado, W.; Perez-Peralta, N.; Islas, R.; Toro-Labbe, A.; Ugalde, J. M.; Merino, G. Designing 3-D Molecular Stars. *J. Am. Chem. Soc.* **2009**, *131*, 9426–9431.

(36) Yao, W.-Y.; Guo, J.-C.; Lu, H.-G.; Li, S.-D. *J. Phys. Chem A* **2009**, *113*, 2561.

(37) Fernandez-Lima, F. A.; VilelaNeto, O. P.; Pimentel, A. S.; Ponciano, C. R.; Pacheco, M. A. C.; Chaer Nascimento, M. A.; da Silviera., E. F. A Theoretical and Experimental Study of Positive and Neutral LiF Clusters Produced by Fast Ion Impact on a Polycrystalline LiF Target. *J. Phys. Chem. A* **2009**, *113*, 1813–1821.

(38) Ortega-Moo, C.; Cervantes, J.; Mendez-Rojas, M. A.; Pannell, K. H.; Merino, G. What is the Structure of $Si_3H_5^-$? *Chem. Phys. Lett.* **2010**, *490*, 1–3.

(39) Bopp, J. C.; Alexandrova, A. N.; Elliott, B. M.; Herden, T.; Johnson, M. A. Vibrational Predissociation Spectra of the O_n^-, n = 3−10, 12 Clusters: Even-Odd Alternation in the Core Ion. *Int. J. Mass Spec.* **2009**, *283*, 94–99.

(40) Alexandrova, A. N.; Boldyrev, A. L.; Li, X.; Sarkas, H. W.; Hendricks, J. H.; Arnold, S. T.; Bowen, K. H. Lithium Cluster Anions: Photoelectron Spectroscopy and Ab Initio Calculations. *J. Chem. Phys.* **2011**, *134*, 044322–044322−8.

(41) Head-Gordon, M.; Pople, J. A.; Frisch, M. J. MP2 Energy Evaluation by Direct Methods. *Chem. Phys. Lett.* **1988**, *153*, 503–506.

(42) Frisch, M. J.; Head-Gordon, M.; Pople, J. A. A Direct MP2 Gradient Method. *Chem. Phys. Lett.* **1990**, *166*, 275–280.

(43) Frisch, M. J.; Head-Gordon, M.; Pople, J. A. Semi-Direct Algorithms for the MP2 Energy and Gradient. *Chem. Phys. Lett.* **1990**, *166*, 281–289.

(44) Cizek, J. On the Use of the Cluster Expansion and the Technique of Diagrams in Calculations of Correlation Effects in Atoms and Molecules. *Adv. Chem. Phys.* **1969**, *14*, 35–89.

(45) Purvis, G. D., III; Bartlett, R. J. A Full Coupled-Cluster Singles and Doubles Model: The Inclusion of Disconnected Triples. *J. Chem. Phys.* **1982**, *76*, 1910–1919.

(46) Scuseria, G. E.; Janssen, C. L.; Schaefer, H. F., III. An Efficient Reformulation of the Closed-Shell Coupled Cluster Single and Double Excitation (CCSD) Equations. *J. Chem. Phys.* **1988**, *89*, 7382–7388.

(47) Scuseria, G. E.; Schaefer, H. F., III. Is Coupled Cluster Singles and Doubles (CCSD) More Computationally Intensive than Quadratic Configuration Interaction (QCISD)? *J. Chem. Phys.* **1989**, *90*, 3700–3703.

(48) Pople, J. A.; Head-Gordon, M.; Raghavachari, K. J. A. Quadratic Configuration Interaction. A General Technique for Determining Electron Correlation Energies. *J. Chem. Phys.* **1987**, *87*, 5968–5975.

(49) Knowles, P. J.; Hampel, C.; Werner, H.-J. Coupled Cluster Theory for High Spin, Open Shell Reference Wave Functions. *J. Chem. Phys.* **1993**, *99*, 5219–5227.

(50) Raghavachari, K.; Trucks, G. W.; Pople, J. A.; Head-Gordon, M. A Fifth-Order Perturbation Comparison of Electron Correlation Theories. *Chem. Phys. Lett.* **1989**, *157*, 479–483.

(51) Hegarty, D.; Robb, M. A. Application of Unitary Group Methods to Configuration Interaction Calculations. *Mol. Phys.* **1979**, *38*, 1795–1812.

(52) Eade, R. H. A.; Robb, M. A. Direct Minimization in MC SCF Theory. The Quasi-Newton Method. *Chem. Phys. Lett.* **1981**, *83*, 362–368.

(53) Schlegel, H. B.; Robb, M. A. MC SCF Gradient Optimization of the $H_2CO \rightarrow H_2$ + CO Transition Structure. *Chem. Phys. Lett.* **1982**, *93*, 43–46.

(54) Bernardi, F.; Bottini, A.; McDougall, J. J. W.; Robb, M. A.; Schlegel, H. B. MC SCF Gradient Calculation of Transition Structures in Organic Reactions. *Faraday Symp. Chem. Soc.* **1984**, *19*, 137–147.

(55) Frisch, M. J.; Ragazos, I. N.; Robb, M. A.; Schlegel, H. B. An Evaluation of Three Direct MC-SCF Procedures. *Chem. Phys. Lett.* **1992**, *189*, 524–528.

(56) Yamamoto, N.; Vreven, T.; Robb, M. A.; Frisch, M. J.; Schlegel, H. B. A Direct Derivative MC-SCF Procedure. *Chem. Phys. Lett.* **1996**, *250*, 373–378.

(57) Schaftenaar, G.; Noordik, J. H. Molden: a pre- and post-processing program for molecular and electronic structures. *J. Comput.-Aided Mol. Design* **2000**, *14*, 123–134.

(58) Schaftenaar, G. *MOLDEN3.4*; CAOS/CAMM Center: The Netherlands, 1998.